

A multi-dimensional sampling method for locating small scatterers

This article has been downloaded from IOPscience. Please scroll down to see the full text article.

2012 Inverse Problems 28 115004

(<http://iopscience.iop.org/0266-5611/28/11/115004>)

View the [table of contents for this issue](#), or go to the [journal homepage](#) for more

Download details:

IP Address: 137.132.123.69

The article was downloaded on 18/10/2012 at 13:33

Please note that [terms and conditions apply](#).

A multi-dimensional sampling method for locating small scatterers

Rencheng Song, Yu Zhong and Xudong Chen

Department of Electrical and Computer Engineering, National University of Singapore, 117576, Singapore

E-mail: elesongr@nus.edu.sg, elezhong@nus.edu.sg and elechenx@nus.edu.sg

Received 29 June 2012, in final form 2 September 2012

Published 28 September 2012

Online at stacks.iop.org/IP/28/115004

Abstract

A multiple signal classification (MUSIC)-like multi-dimensional sampling method (MDSM) is introduced to locate small three-dimensional scatterers using electromagnetic waves. The indicator is built with the most stable part of signal subspace of the multi-static response matrix on a set of combinatorial sampling nodes inside the domain of interest. It has two main advantages compared to the conventional MUSIC methods. First, the MDSM is more robust against noise. Second, it can work with a single incidence even for multi-scatterers. Numerical simulations are presented to show the good performance of the proposed method.

(Some figures may appear in colour only in the online journal)

1. Introduction

Inverse scattering methods have been studied for decades and widely applied in remote sensing [1], through wall imaging [2] and geophysics [3]. The characteristics of scatterers such as location, shape and material property are retrieved from measured scattered fields. The inverse scattering methods can generally be divided into two categories depending on the relative scale of scatterers compared to the wavelength of the illuminating wave. For scatterers of a size comparable with or even larger than the wavelength, there are various quantitative nonlinear iterative methods such as contrast source inversion [4], the Gauss–Newton method [5] and subspace optimization method [6, 7], as well as qualitative non-iterative methods such as linear sampling [8], the factorization method [9] and the direct imaging algorithm [10]. For small scatterers, most methods are qualitative and non-iterative, for example, the decomposition of the time-reversal operator (also called DORT from the French acronym) [11] and the multiple signal classification (MUSIC) method [12–17]. There are also quantitative methods such as the compressive sensing (CS) method [18, 19]. The DORT works well for well-resolved scatterers [14] and it is not a super-resolution imaging algorithm. The CS can work with a

single incidence but requires the measurement matrix to be incoherent [18]. Compared to them, the MUSIC method is simple and works for single frequency data with super-resolution.

As one of the most popular methods to determine the locations of small scatterers, MUSIC defines a pseudo-spectrum function that peaks at the locations of scatterers based on the analysis of the multi-static response (MSR) matrix [20–22]. As is known, the main feature of the time-reversal MUSIC is super-resolution [14]. Namely, the MUSIC method can locate scatterers with separation of less than half a wavelength. The MUSIC method has been successfully applied in acoustic [23, 24], electromagnetic [13, 25] and elastic waves [26, 27]. However, the imaging ability of MUSIC declines dramatically as the noise level increases [24, 28]. In these circumstances, close scatterers appear as a big spot and cannot be distinguished from each other. In [12], an enhanced MUSIC method has been proposed that improves the imaging ability of MUSIC in the presence of moderate noise. On the other hand, compared to methods [18, 19, 29] with a single or few incidences, MUSIC needs multiple incidences, which also limits its application in some practical situations.

In this paper, a MUSIC-like multi-dimensional sampling method (MDSM) is proposed to further increase the robustness against noise as well as to deal with the scattering data with a single incidence. By simultaneously sampling several nodes in the domain of interest, for example, two or more nodes (considered as a combinatorial set) are sampled together, the MDSM is able to construct an indicator using only the most stable part of the signal subspace of the MSR matrix. The more the simultaneously sampled nodes are used, the fewer the number of leading singular vectors needed. In particular, when the dimension of the combinatorial set is equal to the number of unknown scatterers, the MDSM uses only the first leading singular vector of the MSR matrix. This implies that the MDSM is able to work with a single incidence. We should indicate that the idea of sampling on a combinatorial set has also been used in the high-dimensional signal subspace method (HDSSM) [30] which is closely related to maximum likelihood estimation. Compared to conventional MUSIC, the HDSSM has the advantage that it can locate more scatterers with the same measured scattered field. However, this method is very sensitive to noise due to the use of a large number of high-dimensional singular vectors.

To summarize, there are two advantages of the introduced method over the conventional MUSIC methods. First, the MDSM is very stable against noise, due to the use of far fewer leading singular vectors. Second, the proposed method can work with a single incidence. The main drawback of MDSM is its large computational cost compared to the conventional MUSIC method due to the use of combinatorial sets for sampling. Therefore, the MDSM can be considered as a complementary method to MUSIC. Namely, the MDSM can work efficiently on a much smaller domain obtained by MUSIC where the scatterers are most probably present but cannot be separated by MUSIC due to their close distances.

The structure of this paper is as follows. First, in section 2, the forward model of electromagnetic scattering and conventional time-reversal MUSIC methods are briefly reviewed. Then the MDSM is introduced in section 3. Numerical examples are presented in section 4. Finally, conclusions are made in section 5.

2. The forward scattering model and conventional MUSIC methods

In this paper, vectors and matrices are denoted by letters with single and double bars, respectively. Consider M three-dimensional spherical scatterers at $\{\bar{s}_j\}_{j=1}^M$, which are illuminated by electromagnetic waves from N transmitters located at $\{\bar{r}_j\}_{j=1}^N$. Suppose the receivers are coincident with transmitters. Each transceiver consists of three antennas, oriented in the x -, y - and z -directions, respectively. The angular frequency is ω and all materials including background and scatterers are non-magnetic, i.e. $\mu = \mu_0$.

The $3N \times 3N$ MSR matrix is given as [12, 16]

$$\bar{\bar{A}} = \bar{\bar{R}} \cdot \bar{\bar{\Lambda}} \cdot (\bar{\bar{I}} - \bar{\bar{\Phi}} \cdot \bar{\bar{\Lambda}})^{-1} \cdot \bar{\bar{R}}^T, \quad (1)$$

where $\bar{\bar{R}}(i, j) = i\omega\mu_0\bar{\bar{G}}(\bar{r}_i, \bar{s}_j)$, $\bar{\bar{\Lambda}} = \text{diag}(\bar{\bar{\xi}}_1, \bar{\bar{\xi}}_2, \dots, \bar{\bar{\xi}}_M)$, $\bar{\bar{\Phi}}(i, j)$ is null for $i = j$ and otherwise $i\omega\mu_0\bar{\bar{G}}(\bar{s}_i, \bar{s}_j)$, and the superscript T denotes the transpose. $\bar{\bar{I}}$ is a $3M$ -dimensional identity matrix. $\bar{\bar{G}}(\bar{r}_i, \bar{s}_j)$ is the dyadic Green's function in free space [31] and $\bar{\bar{\xi}}_j$ denotes the polarization tensor of the j th scatterer and its expression can be found in [16]. In this paper, all scatterers are supposed to be non-degenerate, which means $\bar{\bar{\xi}}_j$ has full rank for $j = 1, 2, \dots, M$.

The $3N \times 3$ test matrix $\bar{\bar{Q}}(\bar{t}) = [\bar{\bar{G}}^T(\bar{r}_1, \bar{t}), \bar{\bar{G}}^T(\bar{r}_2, \bar{t}), \dots, \bar{\bar{G}}^T(\bar{r}_N, \bar{t})]^T$ is reformulated as $\bar{\bar{Q}}(\bar{t}) = [\bar{Q}_x, \bar{Q}_y, \bar{Q}_z](\bar{t})$, where \bar{t} is an arbitrary test node in the domain of interest and $\bar{Q}_j(\bar{t})$, $j = x, y, z$ represents Green's function vector observed at antennas due to a dipole source at the position \bar{t} oriented in the x -, y -, z -direction, respectively. As is known, the MUSIC method is based on the following theorem.

Theorem 1. Suppose the size of MSR matrix $\bar{\bar{A}}$ is sufficiently large. Let $\bar{a} \in \mathbb{C}^3 \setminus \{0\}$, then

$$\bar{\bar{Q}}(\bar{t}) \cdot \bar{a} \in \mathcal{R}(\bar{\bar{A}}) \quad \text{if and only if} \quad \bar{t} \in \{\bar{s}_j\}_{j=1}^M, \quad (2)$$

where $\mathcal{R}(\bar{\bar{A}})$ denotes the range space of $\bar{\bar{A}}$.

For detailed proof of theorem 1, refer to [6, 12]. Suppose the singular value decomposition (SVD) of the MSR matrix is $\bar{\bar{A}} = \bar{\bar{U}} \cdot \bar{\bar{\Sigma}} \cdot \bar{\bar{V}}^H$, where H denotes the complex conjugate transpose. In a component form, there is $\bar{\bar{A}} \cdot \bar{v}_j = \sigma_j \cdot \bar{u}_j$, $j = 1, 2, \dots, 3N$. As is known, the range space of $\bar{\bar{A}}$ is $\mathcal{R}(\bar{\bar{A}}) = \text{span}\{\bar{u}_j, \sigma_j > 0\}$ with dimension $K = \sum_{i=1}^M \text{rank}(\bar{\bar{\xi}}_j)$. With the MSR matrix, there are also other SVD-based detection and localization techniques, such as [20–22].

The MUSIC method is a qualitative method and its indicator peaks at locations of scatterers. In the standard time-reversal MUSIC method [13], the indicator (pseudo-spectrum function) is defined as

$$W_1(\bar{t}) = \frac{1}{\sum_{i=K+1}^{3N} |\bar{u}_i^H \cdot \bar{\bar{Q}}(\bar{t}) \cdot \bar{a}|^2} \quad (3)$$

$$= \frac{1}{|\bar{\bar{Q}}(\bar{t}) \cdot \bar{a}|^2 - \sum_{i=1}^K |\bar{u}_i^H \cdot \bar{\bar{Q}}(\bar{t}) \cdot \bar{a}|^2}, \quad (4)$$

where $|\cdot|$ denotes the Euclidean distance and \bar{a} is an arbitrarily given test direction.

If there is noise present in the measured scattered fields, the noise is brought into the indicator $W_1(\bar{t})$ by the first K leading singular vectors as seen from (4). We also know that the larger the singular value, the less perturbation the noise causes on its corresponding singular vector. More theoretical analysis on the MSR matrix in the presence of noise can be found in [20–22] using random matrix theory. Therefore, one way to reduce the noise effect is to use only the first few leading singular vectors and their number should be as low as possible. This idea was realized partly in the enhanced MUSIC [12] by choosing an optimal test direction $\bar{a}_{\text{opt}}(\bar{t})$ at each test node \bar{t} instead of a fixed \bar{a} . Here, the optimal test direction is chosen to be the direction $\bar{a}(\bar{t})$ such that $\bar{\bar{Q}}(\bar{t}) \cdot \bar{a}(\bar{t})$ has the smallest angle with a given signal subspace composed of the first L leading singular vectors. Therefore, $\bar{a}_{\text{opt}}(\bar{t})$ satisfies [12]

$$\bar{a}_{\text{opt}}(\bar{t}) = \arg \max_{\bar{a}} \frac{\sum_{i=1}^L |\bar{u}_i^H \cdot \bar{\bar{Q}}(\bar{t}) \cdot \bar{a}|^2}{|\bar{\bar{Q}}(\bar{t}) \cdot \bar{a}|^2}. \quad (5)$$

Correspondingly, the following pseudo-spectrum function [12] is defined:

$$W_2(\bar{t}) = \frac{1}{1 - \cos^2(\theta_{\min}(\bar{t}))}, \quad (6)$$

where $\cos^2(\theta_{\min}(\bar{t})) = \frac{\sum_{i=1}^L |\bar{u}_i^H \bar{\bar{Q}}(\bar{t}) \cdot \bar{a}_{\text{opt}}(\bar{t})|^2}{|\bar{\bar{Q}}(\bar{t}) \cdot \bar{a}_{\text{opt}}(\bar{t})|^2}$ and $\theta_{\min}(\bar{t})$ is the minimal angle that $\bar{\bar{Q}}(\bar{t}) \cdot \bar{a}_{\text{opt}}(\bar{t})$ makes with the subspace $U_L = \text{span}\{\bar{u}_j, j = 1, 2, \dots, L\}$.

Due to the use of the optimal test direction, the number L of leading singular vectors can be reduced from K to $K - 2$, i.e. $L = K - 2$ in the enhanced MUSIC $W_2(\bar{t})$. Compared to $W_1(\bar{t})$ in (4), $W_2(\bar{t})$ keeps a higher resolution against noise. However, it is still vulnerable to noise when the noise level is high because L is still close to K in W_2 .

3. The multi-dimensional sampling method

The MDSM is motivated by an idea similar to the aforementioned enhanced MUSIC and thus it is still referred to as a MUSIC-like method. However, it samples on high-dimensional combinatorial sets of nodes instead of individual physical nodes. Therefore, the number L of singular vectors used to construct the indicator will be further reduced to get a more stable method against noise.

3.1. The theoretical foundation of MDSM

Suppose $\{\bar{t}_1, \bar{t}_2, \dots, \bar{t}_P\}$ is an arbitrary P -dimensional combinatorial set, where \bar{t}_j is an arbitrary test node in the domain of interest and any two of them are not coincident. For a given subspace $U_L (L \leq K)$, the condition that $[\bar{\bar{Q}}(\bar{t}_1), \bar{\bar{Q}}(\bar{t}_2), \dots, \bar{\bar{Q}}(\bar{t}_P)] \cdot \bar{a} \in U_L$ is actually equivalent to finding non-trivial λ_i and \bar{a} such that

$$\sum_{i=1}^L \lambda_i \bar{u}_i = [\bar{\bar{Q}}(\bar{t}_1), \bar{\bar{Q}}(\bar{t}_2), \dots, \bar{\bar{Q}}(\bar{t}_P)] \cdot \bar{a}, \quad (7)$$

where \bar{a} is a $3P$ -dimensional test direction.

We are concerned about the existence of non-trivial \bar{a} and λ_i in (7) for any given combinatorial set $\{\bar{t}_1, \bar{t}_2, \dots, \bar{t}_P\}$ and L -dimensional signal subspace. The answer to this problem implies the principle of MDSM, which is given as follows.

Let $\bar{J}_j^{(i)}$ denote the induced electric current in the j th scatterer corresponding to the i th eigenstate. There is [12]

$$\bar{u}_i = \sum_{j=1}^M \bar{\bar{Q}}(\bar{s}_j) \cdot \bar{J}_j^{(i)}, \quad i = 1, 2, \dots, L. \quad (8)$$

Combining (7) and (8), we have

$$\begin{aligned} \sum_{j=1}^M \bar{\bar{Q}}(\bar{s}_j) \cdot \left(\sum_{i=1}^L \lambda_i \bar{J}_j^{(i)} \right) &= [\bar{\bar{Q}}(\bar{t}_1), \bar{\bar{Q}}(\bar{t}_2), \dots, \bar{\bar{Q}}(\bar{t}_P)] \cdot \bar{a} \\ &= \sum_{k=1}^P \bar{\bar{Q}}(\bar{t}_k) \cdot \bar{a}_k, \end{aligned} \quad (9)$$

where $\bar{a}_k (k \leq P)$ is a three-dimensional vector and $\bar{a} = [\bar{a}_1^T, \bar{a}_2^T, \dots, \bar{a}_P^T]^T$. There are three cases to be considered. (a) No element of the combinatorial set $\{\bar{t}_1, \bar{t}_2, \dots, \bar{t}_P\}$ belongs to $\{\bar{s}_j\}_{j=1}^M$. (b) All elements of the combinatorial set $\{\bar{t}_1, \bar{t}_2, \dots, \bar{t}_P\}$ belong to $\{\bar{s}_j\}_{j=1}^M$. (c) Some elements of the combinatorial set $\{\bar{t}_1, \bar{t}_2, \dots, \bar{t}_P\}$ belong to $\{\bar{s}_j\}_{j=1}^M$.

From theorem 1, we know that vertors of $\{\bar{\bar{Q}}(\bar{t}_l)\}$ are linearly independent for different locations \bar{t}_l . Therefore, for case (a), (9) holds only if $\lambda_i = 0$ and $\bar{a} = 0$. For case (b), suppose $\bar{t}_k = \bar{s}_k$ for $k = 1, 2, \dots, P$. There must be

$$\sum_{i=1}^L \bar{J}_j^{(i)} \lambda_i = \bar{a}_j, \quad j = 1, 2, \dots, P, \quad (10)$$

$$\sum_{i=1}^L \bar{J}_j^{(i)} \lambda_i = 0, \quad j = P+1, P+2, \dots, M. \quad (11)$$

Non-trivial \bar{a}_j exists in (10) if (11) owns non-trivial solution $\{\lambda_i\}_{i=1}^L$. It implies that vectors $\bar{J}^{(i)} = [(\bar{J}_{P+1}^{(i)})^T, (\bar{J}_{P+2}^{(i)})^T, \dots, (\bar{J}_M^{(i)})^T]^T$, $i = 1, 2, \dots, L$ should be linearly dependent. This is true if L is no less than one plus the row number (which physically equals to the total number of independent dipoles that can be excited at scatterers \bar{s}_j , $j = P+1, P+2, \dots, M$) of the matrix $[\bar{J}^{(1)}, \bar{J}^{(2)}, \dots, \bar{J}^{(L)}]$. For example, when all scatterers are non-degenerate, (11) has non-trivial solution when $L \geq 3(M-P)+1$. For case (c), suppose $\bar{t}_1 = \bar{s}_1$ and other $\{\bar{t}_j\}_{j=2}^P$ are not the positions of scatterers. Then \bar{a}_k , $k = 2, 3, \dots, P$, should be zero vectors. The problem is equivalent to discussing case (b) with $P = 1$. The above analysis can be summarized into the following theorem.

Theorem 2. Suppose there are M scatterers. For its arbitrary subset of scatterers with index $\{i_1, i_2, \dots, i_P\}$ ($P \leq M$), there exists an $\bar{a} \in \mathbb{C}^{3P} \setminus \{0\}$ such that

$$[\bar{\bar{Q}}(\bar{s}_{i_1}), \bar{\bar{Q}}(\bar{s}_{i_2}), \dots, \bar{\bar{Q}}(\bar{s}_{i_P})] \cdot \bar{a} \in U_L, \quad (12)$$

where $L \geq Z + 1$ and $Z = \sum_{i \neq \{i_1, i_2, \dots, i_P\}}^M \text{rank}(\bar{\xi}_i)$.

Since we aim to find the minimum eligible L , we choose L to be $Z + 1$. Theorem 2 indicates the condition that \bar{a} exists. It can be seen that L will be reduced if P is increased. Particularly, if $P = M$, i.e. $Z = 0$, \bar{a} exists in theorem 2 when $L = 1$. From theorems 1 and 2, we have the following corollary.

Corollary 3. Suppose the size of MSR matrix $\bar{\bar{A}}$ is sufficiently large. For a given M -dimensional combinatorial set $\{\bar{t}_1, \bar{t}_2, \dots, \bar{t}_M\}$, there exists an $\bar{a} \in \mathbb{C}^{3M} \setminus \{0\}$ such that

$$[\bar{\bar{Q}}(\bar{t}_1), \bar{\bar{Q}}(\bar{t}_2), \dots, \bar{\bar{Q}}(\bar{t}_M)] \cdot \bar{a} \in U_1 \quad \text{if and only if} \quad \bar{t}_j = \bar{s}_j \quad (13)$$

for $j = 1, 2, \dots, M$, where $U_1 = \text{span}\{\bar{u}_1\}$.

Actually, the existence of \bar{a} in corollary 3 can also be obtained by another simple way. Namely,

$$U_1 \subset \mathcal{R}(\bar{\bar{A}}) \subseteq \text{span}\{\bar{Q}_x(\bar{s}_j), \bar{Q}_y(\bar{s}_j), \bar{Q}_z(\bar{s}_j), j = 1, 2, \dots, M\}.$$

Now let us introduce the way to compute \bar{a} in theorem 2. This is also done by the idea of optimal test direction. We denote the test matrix $[\bar{\bar{Q}}(\bar{t}_1), \bar{\bar{Q}}(\bar{t}_2), \dots, \bar{\bar{Q}}(\bar{t}_P)]$ as $\bar{X}(\bar{t}_1, \bar{t}_2, \dots, \bar{t}_P)$. The optimal test direction $\bar{a}_{\text{opt}}(\bar{t}_1, \bar{t}_2, \dots, \bar{t}_P)$ at a combinatorial set $\{\bar{t}_1, \bar{t}_2, \dots, \bar{t}_P\}$ is solved such that the vector $\bar{X}(\bar{t}_1, \bar{t}_2, \dots, \bar{t}_P) \cdot \bar{a}_{\text{opt}}(\bar{t}_1, \bar{t}_2, \dots, \bar{t}_P)$ makes the smallest angle $\theta_{\min}(\bar{t}_1, \bar{t}_2, \dots, \bar{t}_P)$ with a given subspace U_L . Thus, $\bar{a}_{\text{opt}}(\bar{t}_1, \bar{t}_2, \dots, \bar{t}_P)$ satisfies

$$\bar{a}_{\text{opt}}(\bar{t}_1, \bar{t}_2, \dots, \bar{t}_P) = \arg \max_{\bar{a}} \frac{\sum_{i=1}^L |\bar{u}_i^H \cdot \bar{X}(\bar{t}_1, \bar{t}_2, \dots, \bar{t}_P) \cdot \bar{a}|^2}{|\bar{X}(\bar{t}_1, \bar{t}_2, \dots, \bar{t}_P) \cdot \bar{a}|^2}. \quad (14)$$

The $\bar{a}_{\text{opt}}(\bar{t}_1, \bar{t}_2, \dots, \bar{t}_P)$ in (14) is obtained as the eigenvector corresponding to the maximum eigenvalue of matrix $(\bar{X}^H \cdot \bar{X})^{-1}([\bar{U} \cdot \bar{X}]^H \cdot [\bar{U} \cdot \bar{X}])$, where $\bar{U} = [\bar{u}_1, \bar{u}_2, \dots, \bar{u}_L]^H$.

Similar to the enhanced MUSIC, the indicator (pseudo-spectrum function) of MDSM is defined as

$$W_3(\bar{t}_1, \bar{t}_2, \dots, \bar{t}_P) = \frac{1}{1 - \cos^2(\theta_{\min}(\bar{t}_1, \bar{t}_2, \dots, \bar{t}_P))}, \quad (15)$$

where

$$\cos^2(\theta_{\min}(\bar{t}_1, \bar{t}_2, \dots, \bar{t}_P)) = \frac{\sum_{i=1}^L |\bar{u}_i^H \cdot \bar{X}(\bar{t}_1, \bar{t}_2, \dots, \bar{t}_P) \cdot \bar{a}_{\text{opt}}(\bar{t}_1, \bar{t}_2, \dots, \bar{t}_P)|^2}{|\bar{X}(\bar{t}_1, \bar{t}_2, \dots, \bar{t}_P) \cdot \bar{a}_{\text{opt}}(\bar{t}_1, \bar{t}_2, \dots, \bar{t}_P)|^2}.$$

For convenience, we denote the MDSM with L leading singular vectors and P -dimensional combinatorial set as $\text{MDSM}(P, L)$.

3.2. The characteristics of MDSM

In this section, we will discuss the characteristics of MDSM in (15) such as its stability, usage limitation and computational cost. These three issues are discussed one by one in the following.

Firstly, the stability of MDSM against noise is closely related to L . It is worth looking into the physical meaning of \bar{u}_i ($i = 1, 2, \dots, L$) that are used in the indicator function W_3 . The definition of SVD, $\bar{A} \cdot \bar{v}_i = \sigma_i \cdot \bar{u}_i$, actually shows that \bar{u}_i is the measured scattering data when the transmitting antennas are loaded with current \bar{v}_i/σ_i , $i = 1, 2, \dots, L$. Thus, in the indicator function (15), a total number of L scattering experiments are conducted, with \bar{u}_1 the most stable and \bar{u}_L the least stable. As shown in corollary 3, one is able to locate all the scatterers with only the first singular vector which is the most stable against noise compared to other ones. However, in MDSM with $L = 1$, its resolution is strictly limited by the noise level of the first singular vector. In other words, only one scattering experiment is conducted, i.e. only one incidence with \bar{v}_1/σ_1 as the driving current.

In comparison, when L is chosen as larger than 1, a trade-off between the following two factors has to be taken into account. One is that from the second incidence onwards, experimental results gradually become less stable. The other is that we have more scattering data at hand since several experiments have been conducted. A simultaneous use of all experimental data may reduce the effect of error that is contained in each individual experiment, including the first one. Obviously, whereas the first factor favors a small value of L , the second one favors a reasonably large L . All our numerical simulations conducted so far show the optimal value of L , that is, $1 \leq L \leq 3$. In this case ($L \leq 3$), there is only a single peak corresponding to the scatterer positions appearing in MDSM.

Secondly, when $L \leq 3$, the MDSM needs to do sampling with M -dimensional combinatorial sets. It means that prior information that $P = M$ is required. Therefore, the MDSM is used in two ways depending on whether M is known or not. If M is known, we directly make use of $\text{MDSM}(M, L \leq 3)$. Otherwise, a strategy of using MDSM with $L \leq 3$ recursively from low ($P = 1$) to high dimension is necessary. It can be easily determined when P reaches M . Namely, by theorem 2, the number of peaks changes from zero, one to multiple successively with $P = M - 1$, $P = M$ and $P = M + 1$. We mention in passing that the $\text{MDSM}(M + 1, L \leq 3)$ peaks at each combinatorial set $\{\bar{s}_1, \bar{s}_2, \dots, \bar{s}_M, \bar{t}_l\}$ with \bar{t}_l an arbitrary non-scatterer location. The change in the number of peaks is a simple and effective indicator in determining the total number M of scatterers.

Thirdly, the MDSM(P, L) needs to do sampling with P -dimensional combinatorial sets. Suppose there are Y individual nodes in the domain of interest. The total number of combinatorial sets is C_Y^P which is very large when Y and P are large. The computational cost of MDSM can be reduced by using smaller Y and P . For reducing Y , the MDSM is suggested to be used as a post-processing method after the pre-screening by MUSIC methods. Namely, the MDSM is applied to those sub-domains where scatterers are shown to be present as displayed in the MUSIC pseudo-spectrum. Thus, the total number Y can be reduced effectively. For reducing P , an extreme case is the MDSM with $P = 1$ which is just the enhanced MUSIC in [12]. However, the cost is that we need to increase L simultaneously, which may deprave the stability of the MDSM. To summarize, whereas the MUSIC, which can be regarded as a special case of the MDSM with $P = 1$, is most computationally economic, the imaging results are least stable in the presence of noise. On the other extreme, the MDSM with $P = M$ is most computationally expensive, but it yields most stable imaging results in the presence of noise. Thus, if the noise level is moderate, the MDSM with $1 < P < M$ may achieve a good compromise between stability and computational cost.

Different from $L \leq 3$, a lot of peaks may appear in MDSM(P, L) with $L > 3$. From theorem 2, for a given P -dimensional combinatorial set containing at least one scatterer, whether the peak will appear or not is determined by the value of L . For example, suppose there are three non-degenerate scatterers. The rank of the MSR matrix is 9. When $L = 4$ and $P = 2$, there will be three peaks for MDSM(2,4), i.e. any combination of two out of the three scatterers leads to a peak in the pseudo-spectrum. If we increase L , for example $L = 7$, in addition to the existing three peaks, MDSM(2,7) produces many other peaks, which occur at each two-dimensional combinatorial set composed of one scatterer position with another non-scatterer position.

In this paper, we are interested in reconstructing small scatterers in the presence of high-level noise where the conventional MUSIC struggles. Thus, we only use the MDSM with $L \leq 3$. According to the above analysis, in figure 1, we give a flowchart to show the use of MDSM in practice.

3.3. The MDSM with a single incidence

As shown in corollary 3, the MDSM works for only a single incidence if M -dimensional combinatorial sets are taken for sampling. Next we introduce the details for this case.

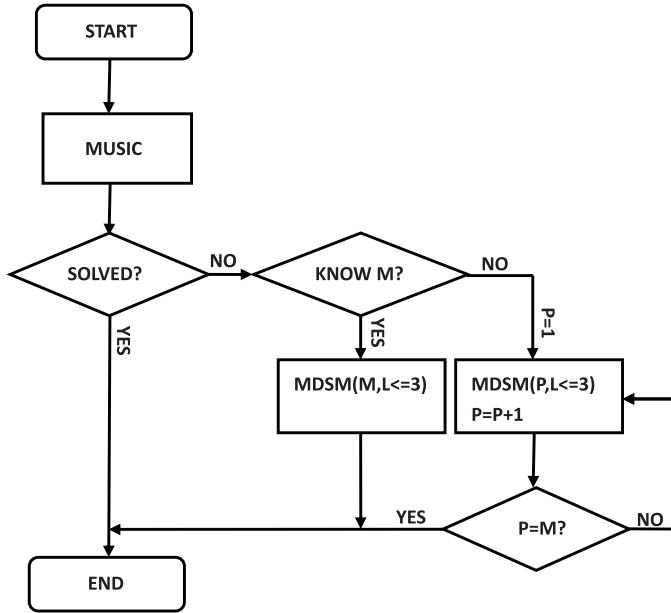
Each column of $\bar{\bar{A}}$ in (1) corresponds to the scattered field due to a single incidence. For example,

$$\bar{A}_j = \bar{\bar{A}}(:, j) = [\bar{\bar{Q}}(\bar{s}_1), \bar{\bar{Q}}(\bar{s}_2), \dots, \bar{\bar{Q}}(\bar{s}_M)] \cdot \bar{\alpha}(j) \quad (16)$$

is the measured scattered field due to the j th incidence, where $\bar{\alpha}(j) = i\omega\mu_0\bar{\Lambda} \cdot (\bar{I} - \bar{\Phi} \cdot \bar{\Lambda})^{-1} \cdot \bar{R}^T(:, j)$. All scatterers can be located by applying the MDSM($M, 1$) with \bar{A}_j . The first singular vector \bar{u}_1 of \bar{A}_j (which is now considered as a special matrix with a single column) is simply the normalized scattered field $\bar{A}_j/|\bar{A}_j|$.

Compared to the MDSM($M, 1$) with full incidences (namely $\bar{\bar{A}}$ in (1)), the MDSM($M, 1$) with single incidence (\bar{A}_j in (16)) has the advantage of less measurement cost but at the same time has the disadvantage in the stability against noise. This is because the SVD has an effect of denoise. It can extract a synthetic normalized scattered field (namely the first leading singular vector) with less noise from more measurement.

Because of this reason, taking more than one incidence usually leads to a much better result than a single incidence. Suppose there are l incidences. For example, the $\{j_1, j_2, \dots, j_l\}$ th

**Figure 1.** A flowchart of the use of the MDSM.

columns of the scattered field are chosen from the MSR matrix $\bar{\bar{A}}$ in (1). There is

$$\bar{\bar{A}}_{j_1, j_2, \dots, j_l} = [\bar{\bar{A}}(:, j_1), \bar{\bar{A}}(:, j_2), \dots, \bar{\bar{A}}(:, j_l)] \quad (17)$$

$$= [\bar{\bar{Q}}(\bar{s}_1), \bar{\bar{Q}}(\bar{s}_2), \dots, \bar{\bar{Q}}(\bar{s}_M)] \cdot [\bar{\alpha}(j_1), \bar{\alpha}(j_2), \dots, \bar{\alpha}(j_l)]. \quad (18)$$

The MDSM($M, 1$) can be applied with the above $\bar{\bar{A}}_{j_1, j_2, \dots, j_l}$ instead of $\bar{\bar{A}}$ to locate all the scatterers. Usually, two or three incidences are enough to get satisfactory results. Here, L can also be relaxed to $L \leq 3$ if the number of incidences is large enough, which is helpful to confirm the validity of the results obtained by the MDSM with $L = 1$.

4. Numerical simulations

In this section, the proposed method is tested through numerical simulations. Two examples are considered, the MDSM with multiple incidences and the MDSM with a single (or few) incidence(s). The experimental configuration is introduced first. Suppose the working frequency is 300 MHz. The background medium is air with permittivity and permeability ϵ_0 and μ_0 , respectively.

Example 1: Three close scatterers with full incidences

In this example, three scatterers with locations at $\bar{s}_1 = (-0.1166, -0.0047, -0.0167)\lambda_0$, $\bar{s}_2 = (0.0611, 0.1730, -0.0167)\lambda_0$ and $\bar{s}_3 = (-0.0278, 0.0842, 0.1610)\lambda_0$, respectively, are considered, where λ_0 is the wavelength of free space. The minimal distance between these three scatterers is $0.218\lambda_0$ and the largest distance is $0.251\lambda_0$. The accurate locations of scatterers for example 1 are shown in figure 2(a). Their permittivities are $\bar{\epsilon}_1 = \text{diag}(2\epsilon_0, 2\epsilon_0, 2\epsilon_0)$,

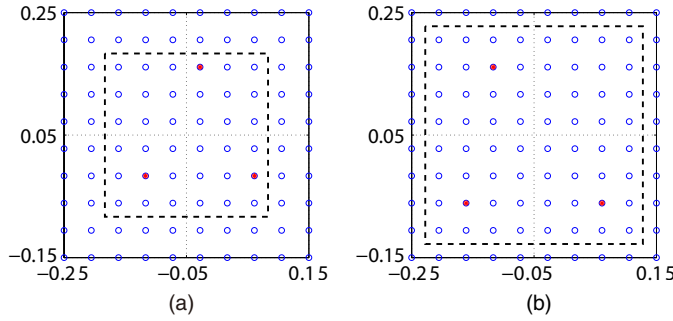


Figure 2. Accurate locations of scatterers. (a) Example 1. (b) Example 2.

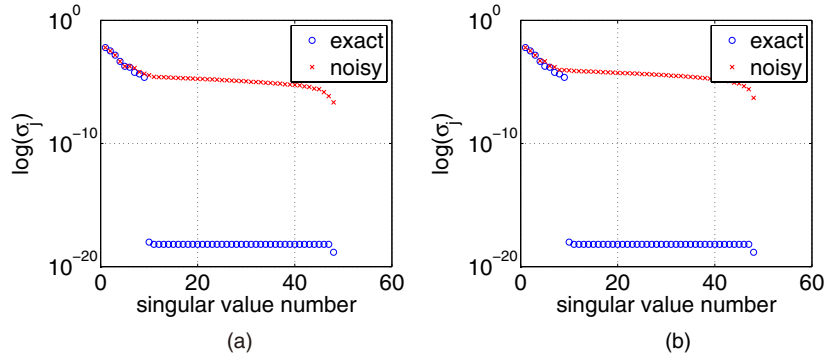


Figure 3. Singular values of the MSR matrix. (a) Singular values with 30 dB Gaussian white noise ($j = 1, 2, \dots, 48$). (b) Singular values with 20 dB Gaussian white noise ($j = 1, 2, \dots, 48$).

$\bar{\epsilon}_2 = \text{diag}(2\epsilon_0, 2\epsilon_0, 2\epsilon_0)$ and $\bar{\epsilon}_3 = \text{diag}(2\epsilon_0, 3\epsilon_0, 4\epsilon_0)$, respectively. The Euler angles are set as $[\frac{\pi}{4}, \frac{\pi}{3}, \frac{3\pi}{8}]$. The test domain is chosen to be a square domain $[-0.25, 0.15]\lambda_0 \times [-0.15, 0.25]\lambda_0$ centered at $(0, 0, 0)$ on the $y = x + 0.112\lambda_0$ plane. All these three scatterers have radius $a = \frac{\lambda_0}{30}$. There are 16 receivers (transmitters are coincident with these receivers) located at the $x = -13\lambda_0$ plane. Half of the receivers are along the y -axis, while the rest are along the z -axis where they are centered at $(-13, -9, 11)\lambda_0$ and the two neighboring cells are at distance $5\lambda_0$.

Let us first consider MUSIC methods in the noise-contaminated case. Gaussian white noises of 30 and 20 dB [12] are added to the MSR matrix, respectively. The singular values of the MSR matrix are shown in figure 3. It can be seen that the rank of the noiseless MSR matrix is 9 and the small singular values change a lot due to noise, especially when the noise level is high. The results of standard time-reversal MUSIC $W_1(\bar{t})$ as well as the enhanced MUSIC $W_2(\bar{t})$ are shown in figure 4. Here $K = 9$ and $L = 7$ are used in $W_1(\bar{t})$ and $W_2(\bar{t})$, respectively. It can be seen that both the MUSIC methods fail to locate any of the scatterers due to the influence of noise. Indeed, the problem is challenging since the three scatterers are very closely located. All three scatterers mix together and become a large spot. It illustrates that the MUSIC method cannot get satisfactory results when noise is high.

Next, we consider the MDSM for example 1. To verify the theoretical analysis in section 3.2, we first show the results of MDSM($P, 1$) in the noise-free case. Suppose the number of scatterers M is unknown. According to the flowchart in figure 1, the MDSM is

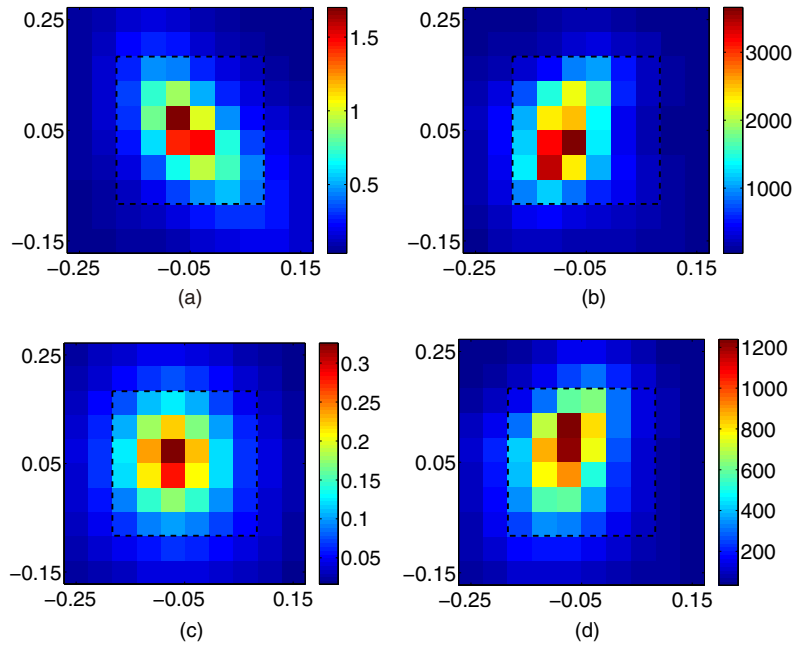


Figure 4. Pseudo-spectra of the standard and enhanced MUSIC methods under different noise levels. (a) Standard MUSIC with 30 dB noise. (b) Enhanced MUSIC with 30 dB noise. (c) Standard MUSIC with 20 dB noise. (d) Enhanced MUSIC with 20 dB noise.

applied from low ($P = 1$) to high dimension ($P = 4$) in the sub-domain (as seen in the region surrounded by the dashed line in figure 2(a)) obtained by MUSIC. The corresponding results of MDSM are shown in figure 5. Here, small circular marker indicates the pseudo-spectrum value at each combinatorial set, while the peaks (with values larger than 10^{14}) are marked by a plus sign. It can be seen that the pseudo-spectrum values jump several orders of magnitude when P changes from 2 to 3. A single peak appears when $P = 3$, as shown in figure 5(c). This means that the number of scatterers is 3. When further increasing P to 4, 33 peaks (the peak number of MDSM($M + 1, 1$) is equal to $Y - M$; here $Y = 36$ is the total physical nodes in the domain of interest) appear, as shown in figure 5(d). It further ensures our analysis on the number of scatterers. All these results are consistent with the theoretical analysis in section 3.2.

Then, we consider the noise-contaminated case of MDSM for example 1. For this case, if the number M of scatterers is unknown, the way to determine M in MDSM is same as the above noise-free case. It still can be determined by the multi-fold procedure as shown in figure 6. It is seen that the maximal magnitude of pseudo-spectra increases significantly with P for $P \leq M$ ($M = 3$ here) and it retains the same level (10^4 for this example) when $P = M + 1 (= 4)$. Then $M = 3$ is confirmed. Therefore, in the following, we only show the results of MDSM with $P = M$ ($P = 3$ here). In order to intuitively judge the accuracy of the results, the exact index of combinatorial set is marked with a small square marker, as seen in figure 7. It is observed that both results of the MDSM(3,1) and MDSM(3,2) with 30 dB noise are accurate. However, the peak with $L = 2$ is much higher and more obvious than $L = 1$. Although not shown here, the result of $L = 3$ is similar to the result of $L = 2$. It confirms that the result of $L = 1$ is reliable. When noise is increased to 20 dB, we can see from figure 7(c) the MDSM(3,1) still works but the highest peak is not outstanding among others. In this case,

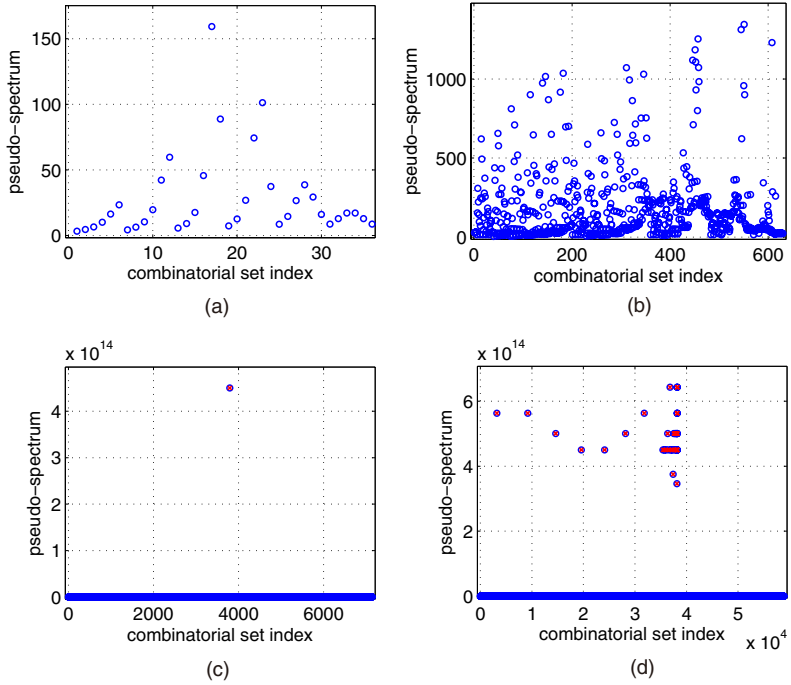


Figure 5. Pseudo-spectra of the MDSM ($L = 1$) in noise-free case with different dimensions of combinatorial sets. (a) MDSM(1,1). (b) MDSM(2,1). (c) MDSM(3,1). (d) MDSM(4,1).

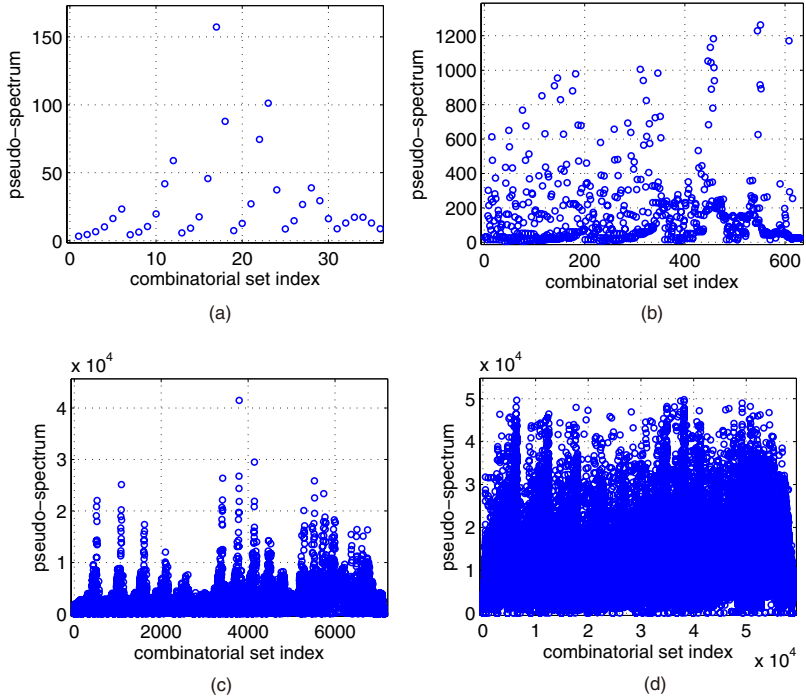


Figure 6. Pseudo-spectra of MDSM ($L = 1$) with different dimensions of combinatorial sets under 30 dB Gaussian white noise. (a) MDSM(1,1). (b) MDSM(2,1). (c) MDSM(3,1). (d) MDSM(4,1).

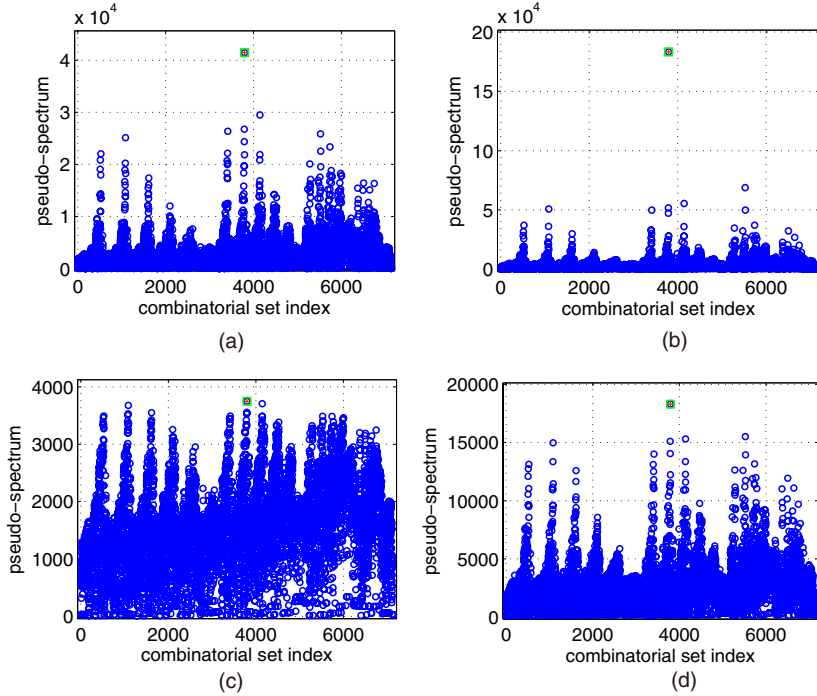


Figure 7. Pseudo-spectra of the MDSM under different noise levels. (a) MDSM(3,1) with 30 dB noise. (b) MDSM(3,2) with 30 dB noise. (c) MDSM(3,1) with 20 dB noise. (d) MDSM(3,2) with 20 dB noise.

comparing the results with the MDSM(3,2) and MDSM(3,3) helps to verify the validity of the obtained results, as shown in figure 7(d). These results in figure 7 show that the MDSM works well with high noise.

Example 2: Three close scatterers with a single incidence

In the second example, we consider the MDSM with a single or few incidences. Suppose there are three scatterers with locations at $\bar{s}_1 = (-0.1610, -0.0491, -0.0611)\lambda_0$, $\bar{s}_2 = (-0.1166, -0.0047, 0.1610)\lambda_0$ and $\bar{s}_3 = (0.0611, 0.1730, -0.0611)\lambda_0$. The accurate locations of scatterers for example 2 is shown in figure 2(b). The smallest distance between them is $0.231\lambda_0$, while the largest distance is $0.336\lambda_0$. Other parameters are the same as that in the first example.

To verify the validity of MDSM with a single incidence, noise-free results of the MDSM are first given in figure 8(a). It can be seen that the MDSM works perfectly with the first incidence without noise. In a noise-contaminated case, where 30 dB Gaussian white noise is added to the measured scattered field, the pseudo-spectra of MDSM with different numbers of incidences are illustrated in figures 8(b)–(f). The results of MDSM with the 11th incidence are shown in figure 8(b), where the highest peak corresponds to the exact index of the combinatorial set. In comparison, we see in figures 8(c) and (e) that taking two (the 11th and 23rd) or three (the 11th, 23rd and 47th) incidences helps to get a sharper peak, which is necessary when noise in the measured scattered field due to a single incidence is too high. This is reasonable because multiple incidences are helpful in obtaining a more stable leading singular vector

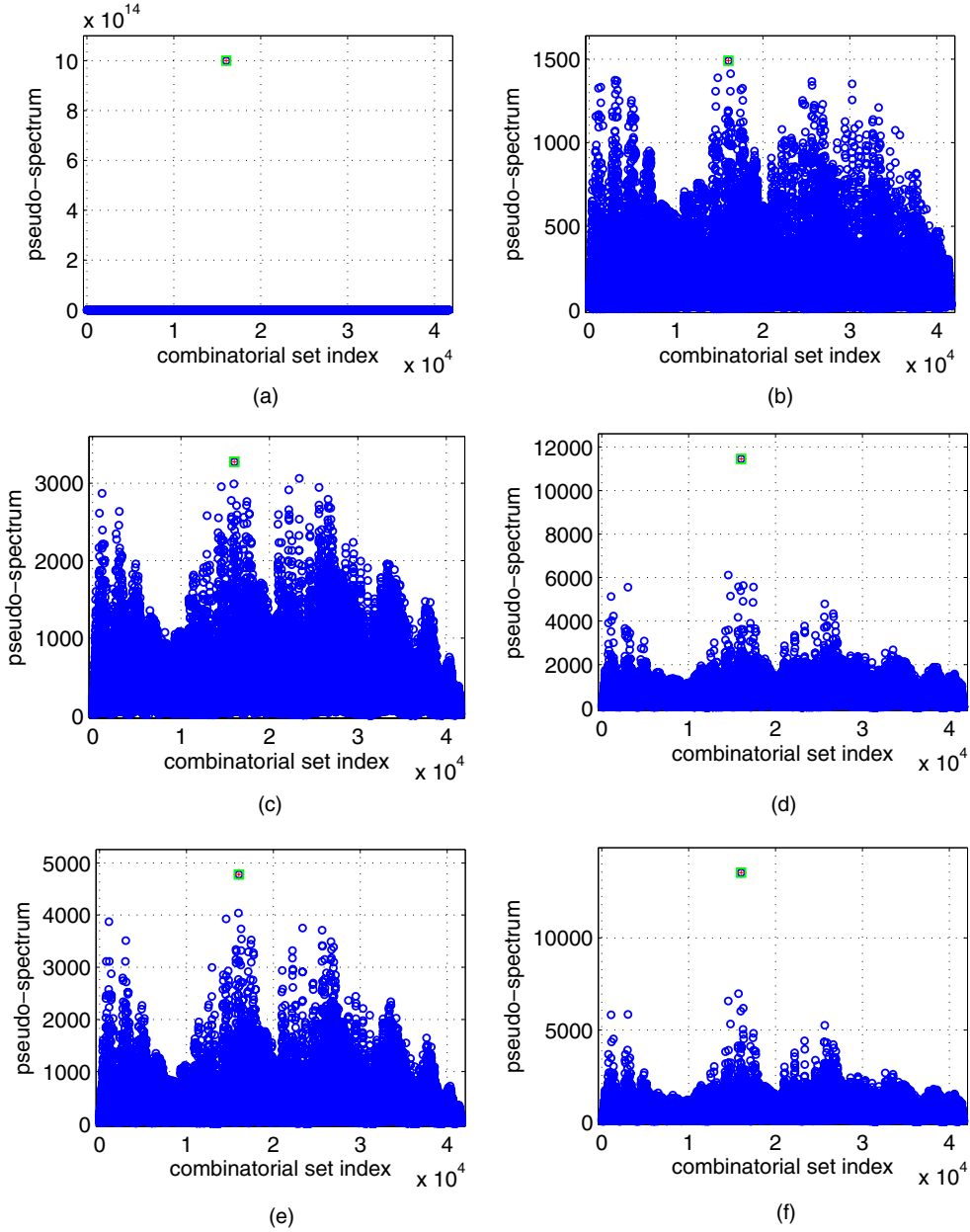


Figure 8. Pseudo-spectra of the MDSM with different numbers of incidences, where (a) is noise-free and others ((b)–(f)) are under 30 dB Gaussian white noise. (a) MDSM(3,1) with the first incidence. (b) MDSM(3,1) with the 11th incidence. (c) MDSM(3,1) with the 11th and 23rd incidences. (d) MDSM(3,2) with the 11th and 23rd incidences. (e) MDSM(3,1) with the 11th, 23rd and 47th incidences. (f) MDSM(3,2) with the 11th, 23rd and 47th incidences.

than a single incidence. At the same time, the results of the MDSM with $L = 2$ for two or three incidences are also given in figures 8(d) and (f), respectively, which further confirm the validity of the results obtained by the MDSM with $L = 1$. Therefore, as shown in figure 8, making use of two or three incidences rather than a single incidence improves the stability of

the MDSM. Of course, if noise is too high, an extreme case is to use the MDSM with full incidences to obtain satisfactory results.

5. Conclusions

In this paper, we have introduced the MDSM to locate small 3D scatterers, which can be seen as a generalization of conventional MUSIC methods. It shares the theoretical foundation of MUSIC (theorem 1) but has special advantages due to the use of the optimal test direction (theorem 2). Numerical simulations verify the advantages of the proposed method over the known time-reversal MUSIC methods. Namely the MDSM is more robust against noise and is capable of working with a single or a small number of incidences. The drawback of the MDSM is its large computational cost because of the use of combinatorial sampling sets. Therefore, the MDSM can be considered as a complementary method of MUSIC, since it is suitable for locating a low number of scatterers inside a small domain of interest. Finally, although the MDSM is introduced for electromagnetic waves in this paper, it can also be easily extended to acoustic or elastic waves.

Acknowledgments

This work was supported by the Singapore Temasek Defence Systems Institute under grant TDSI/10-005/1A.

References

- [1] Hansen T and Johansen P 2000 Inversion scheme for monostatic ground penetrating radar that takes into account the planar air–soil interface *IEEE Trans. Geosci. Remote Sens.* **38** 496–506
- [2] Song L, Yu C and Liu Q 2005 Through-wall imaging (TWI) by radar: 2D tomographic results and analyses *IEEE Trans. Geosci. Remote Sens.* **43** 2793–8
- [3] Zhdanov M and Hursan G 2000 3D electromagnetic inversion based on quasi-analytical approximation *Inverse Problems* **16** 1297–322
- [4] Abubakar A, Hu W, van den Berg P and Habashy T 2008 A finite-difference contrast source inversion method *Inverse Problems* **24** 065004
- [5] Mojabi P and LoVetri J 2009 Overview and classification of some regularization techniques for the Gauss–Newton inversion method applied to inverse scattering problems *IEEE Trans. Antennas Propag.* **57** 2658–65
- [6] Chen X, Zhong Y and Agarwal K 2010 Subspace methods for solving electromagnetic inverse scattering problems *Methods Appl. Anal.* **17** 407–32
- [7] Zhong Y and Chen X 2009 Two-fold subspace-based optimization method for solving inverse scattering problems *Inverse Problems* **25** 085003
- [8] Colton D, Haddar H and Piana M 2003 The linear sampling method in inverse electromagnetic scattering *Inverse Problems* **19** S105
- [9] Kirsch A 2004 The factorization method for Maxwell’s equations *Inverse Problems* **20** S117
- [10] Hou S, Sølna K and Zhao H 2006 A direct imaging algorithm for extended targets *Inverse Problems* **22** 1151–78
- [11] Prada C, Manneville S, Spoliansky D and Fink M 1996 Decomposition of the time reversal operator: detection and selective focusing on two scatterers *J. Acoust. Soc. Am.* **99** 2067–76
- [12] Chen X and Zhong Y 2009 MUSIC electromagnetic imaging with enhanced resolution for small inclusions *Inverse Problems* **25** 015008
- [13] Ammari H, Iakovleva E, Lesselier D and Perrusson G 2007 MUSIC-type electromagnetic imaging of a collection of small three-dimensional bounded inclusions *SIAM J. Sci. Comput.* **29** 674–709
- [14] Devaney D 2005 Time reversal imaging of obscured targets from multistatic data *IEEE Trans. Antennas Propag.* **53** 1600–10
- [15] Marengo E, Hernandez R and Lev-Ari H 2007 Intensity-only signal-subspace-based imaging *J. Opt. Soc. Am. A* **24** 3619–35
- [16] Zhong Y and Chen X 2007 MUSIC imaging and electromagnetic inverse scattering of multiple-scattering small anisotropic spheres *IEEE Trans. Antennas Propag.* **55** 3542–9

- [17] Ammari H, Iakovleva E and Lesselier D 2005 A MUSIC algorithm for locating small inclusions buried in a half-space from the scattering amplitude at a fixed frequency *Multiscale Model. Simul.* **3** 597–628
- [18] Fanjiang A 2010 Compressive inverse scattering: I. High-frequency SIMO/MISO and MIMO measurements *Inverse Problems* **26** 035008
- [19] Fanjiang A 2010 Compressive inverse scattering: II. Multi-shot SISO measurements with Born scatterers *Inverse Problems* **26** 035009
- [20] Ammari H, Garnier J and Jugnon V 2011 Detection, reconstruction, and characterization algorithms from noisy data in multistatic wave imaging, submitted
- [21] Ammari H, Garnier J, Kang H, Park W K and Sølna K 2011 Imaging schemes for perfectly conducting cracks *SIAM J. Appl. Math.* **71** 68–91
- [22] Ammari H, Garnier J and Sølna K 2012 A statistical approach to target detection and localization in the presence of noise *Waves Random Complex Media* **22** 40–65
- [23] Chen X 2010 Multiple signal classification method for detecting point-like scatterers embedded in an inhomogeneous background medium *J. Acoust. Soc. Am.* **127** 2392–7
- [24] Ammari H, Garnier J, Jugnon V and Kang H 2011 Direct reconstruction methods in ultrasound imaging of small anomalies *Lect. Notes Math.* **2035** 31–56
- [25] Song R, Chen R and Chen X 2012 Imaging three-dimensional anisotropic scatterers in multilayered medium by multiple signal classification method with enhanced resolution *J. Opt. Soc. Am. A* **29** 1900–5
- [26] Ammari H, Calmon P and Iakovleva E 2008 Direct elastic imaging of a small inclusion *SIAM J. Imaging Sci.* **1** 169–87
- [27] Song R, Chen X and Zhong Y 2012 Imaging small three-dimensional elastic inclusions by an enhanced multiple signal classification method *J. Acoust. Soc. Am.* **132** 2420–6
- [28] Ammari H, Garnier J, Jugnon V and Kang H 2012 Stability and resolution analysis for a topological derivative based imaging functional *SIAM J. Control Optim.* **50** 48–76
- [29] Ito K, Jin B and Zou J 2012 A direct sampling method to an inverse medium scattering problem *Inverse Problems* **28** 025003
- [30] Marengo E and Gruber F 2007 Subspace-based localization and inverse scattering of multiply scattering point targets *EURASIP J. Adv. Signal Process.* **2007** 17342
- [31] Kong J A 2000 *Electromagnetic Wave Theory* (Cambridge, MA: EMW)